

# **Electronic Supplementary Information (ESI)**

## **Exploration of Charge Transport Materials to Improve the Radiation Tolerance of Lead Halide Perovskite Solar Cells**

Yoshiyuki Murakami,<sup>a</sup> Ryosuke Nishikubo,<sup>a, b</sup> Fumitaka Ishiwari,<sup>a, b</sup> Kazumasa Okamoto,<sup>c</sup>

Takahiro Kozawa<sup>c</sup> and Akinori Saeki\*,<sup>a, b</sup>

<sup>a</sup>Department of Applied Chemistry, Graduate School of Engineering, Osaka University, 2-1 Yamadaoka, Suita, Osaka 565-0871, Japan.

<sup>b</sup>Innovative Catalysis Science Division, Institute for Open and Transdisciplinary Research Initiatives (ICS-OTRI), Osaka University, 1-1 Yamadaoka, Suita, Osaka 565-0871, Japan

<sup>c</sup>SANKEN, Osaka University, 8-1 Mihogaoka, Ibaraki, Osaka 567-0047, Japan.

**Supplementary Tables S1–S2**

**Supplementary Figure S1–S16**

**Supplementary Reference S1**

**Table S1.** Normalized  $\varphi \Sigma \mu_{\max}$  and  $\tau$  (lifetime) of EB ( $2.5 \times 10^{15} \text{ cm}^{-2}$ )-exposed films relative to those without EB exposure.

HTM or ETM	Normalized $\varphi \Sigma \mu_{\max}$	$\tau^{\text{a}}$
C <sub>60</sub>	0.70±0.07	1.08±0.11
PCBM	0.65±0.10	0.97±0.41
CuSCN	0.55±0.10	0.59±0.07
PTB7	0.85±0.12	0.99±0.06
PTAA	0.70±0.08	0.98±0.15

<sup>a</sup> The  $\tau$  was obtained by fitting the double exponential functions ( $A_1 \exp(-t/\tau_1) + A_2 \exp(-t/\tau_2)$ ) to the kinetics and calculating the effective lifetimes ( $\tau = (A_1\tau_1 + A_2\tau_2)(A_1 + A_2)^{-1}$ ). The values are normalized by  $\tau$  before EB exposure.

**Table S2.** EB effect on hole transport yield (TiO<sub>2</sub>/Perovskite/PTB7 or PTAA).<sup>a</sup>

HTM	EB exposure	$\eta_0$	$\eta_{\text{sat}}$	$k (\text{s}^{-1})$
PTB7	Before EB	0.33	0.96	$1.26 \times 10^6$
	After EB ( $F_{\text{EB}} = 2.5 \times 10^{15} \text{ cm}^{-2}$ )	0.22	0.58	$8.64 \times 10^4$
PTAA	Before EB	0.21	0.95	$1.51 \times 10^6$
	After EB ( $F_{\text{EB}} = 2.5 \times 10^{15} \text{ cm}^{-2}$ )	0.28	0.93	$7.55 \times 10^5$

<sup>a</sup>  $\eta_0$ ,  $\eta_{\text{sat}}$ , and  $k$  were obtained from the analysis of decay fitting. The details are reported in the literature.<sup>S1</sup>

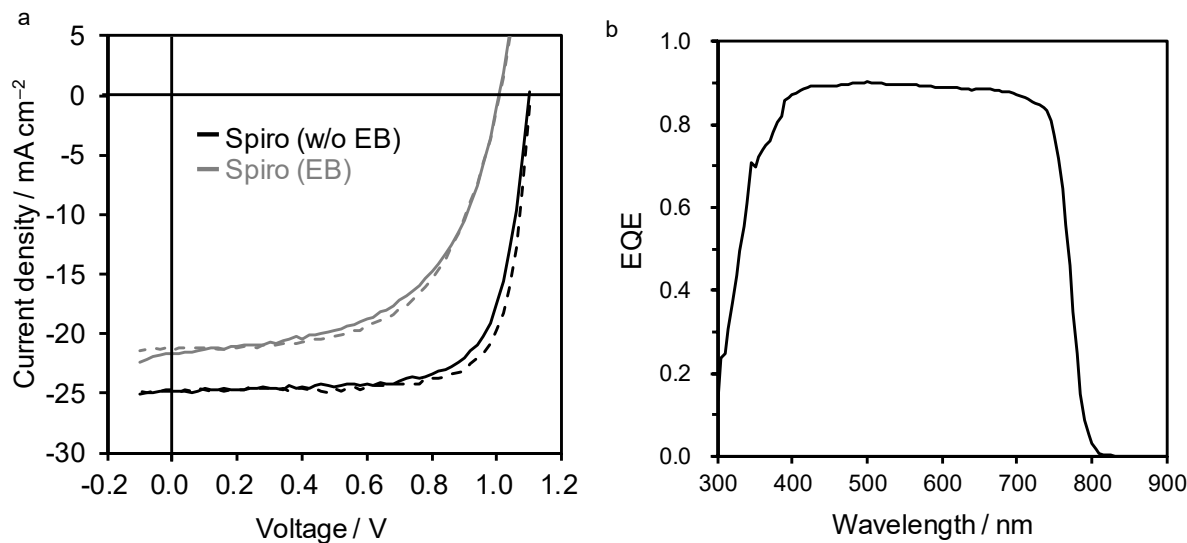


**Figure S1.** (a) JV curves of Device 1 (FTO/c-TiO<sub>2</sub>/mpTiO<sub>2</sub>/PVK/Spiro-OMeTAD/Au) without EB exposure (black lines) and after  $2.5 \times 10^{15} \text{ cm}^{-2}$  exposure (gray lines). The solid and dotted lines are the forward and reverse scans, respectively. (b) EQE spectrum of Device 1 without EB. The maximum value is 0.90 at  $\sim 500 \text{ nm}$ , and the onset is  $\sim 815 \text{ nm}$ . The  $J_{\text{SC}}$  calculated by integrating the EQE spectrum is  $22.1 \text{ mA cm}^{-2}$ , which is smaller than the  $J_{\text{SC}}$  under 1 sun ( $25.3 \text{ mA cm}^{-2}$ ; 13% difference). Note that the light intensities of our EQE instrument and solar simulator were calibrated by a standard cell, and a good match ( $\pm 2\%$  difference) is obtained for organic solar cells. The small  $J_{\text{SC}}$  in EQE of PSC may be due to the trap filling under a stronger white light intensity of a solar simulator (our EQE facility does not provide a white light bias, and thus, the EQE is measured upon the exposure to a weaker intensity of light).

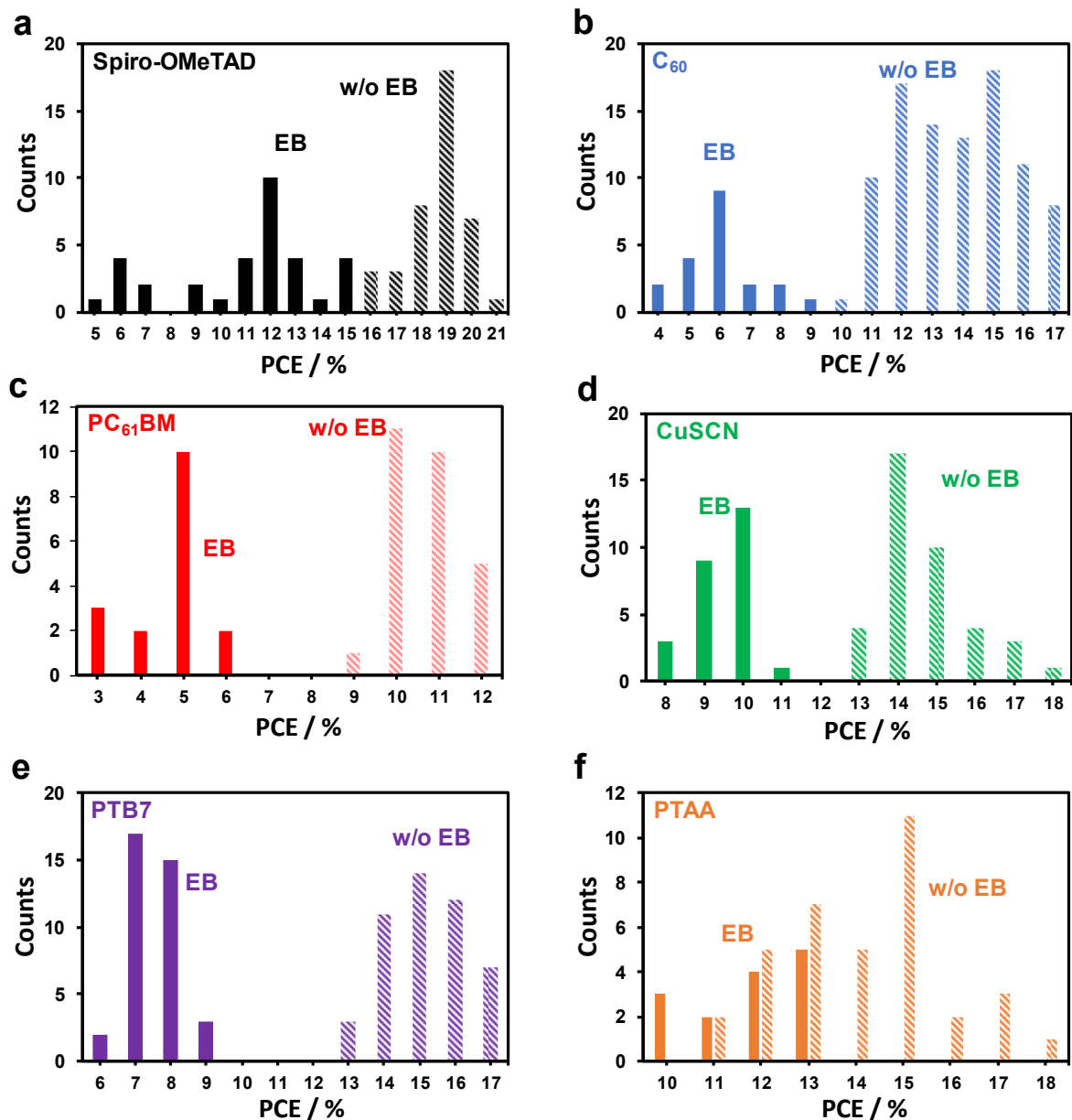


**Figure S2.** Histograms of the PCE values of each PSC without EB exposure (solid bar) and after  $2.5 \times 10^{15} \text{ cm}^{-2}$  exposure (meshed bar). (a) Spiro-OMeTAD (b)  $\text{C}_{60}$  (c) PCBM (d) CuSCN (e) PTB7 (f) PTAA.

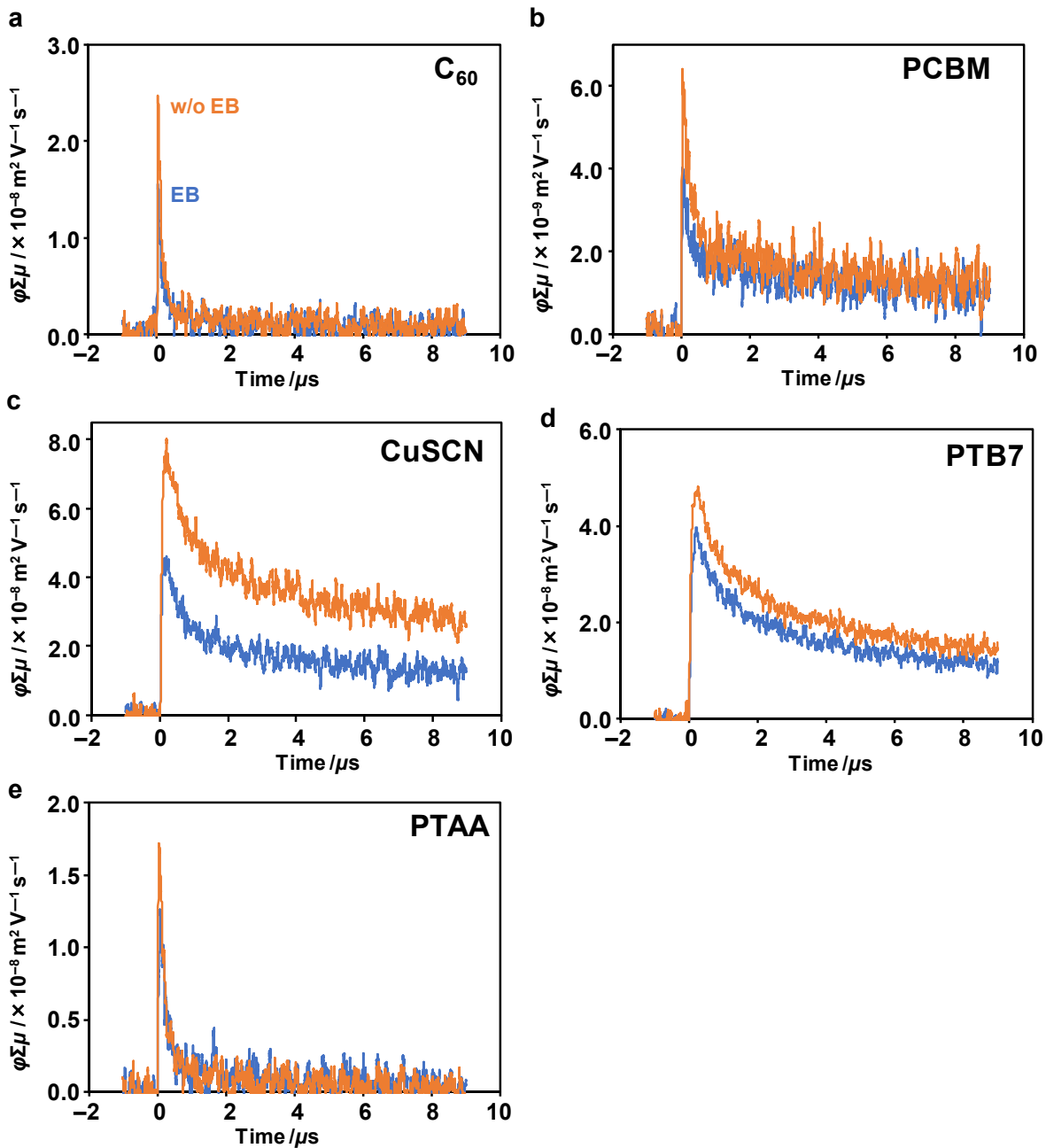


**Figure S3.** TRMC transients ( $\lambda_{\text{ex}} = 355 \text{ nm}$ ) of (a)  $\text{C}_{60}$  (b)  $\text{PC}_{61}\text{BM}$  (c)  $\text{CuSCN}$  (d)  $\text{PTB7}$  (e)  $\text{PTAA}$  with EB exposure of  $2.5 \times 10^{15} \text{ cm}^{-2}$  (blue line) and without EB exposure (orange line). Photon density  $I_0 = 7.0 \times 10^{15} \text{ photons cm}^{-2} \text{ pulse}^{-1}$  ( $\text{C}_{60}$ ),  $1.3 \times 10^{16} \text{ photons cm}^{-2} \text{ pulse}^{-1}$  ( $\text{PTAA}$ ), or  $2.0 \times 10^{16} \text{ photons cm}^{-2} \text{ pulse}^{-1}$  ( $\text{PCBM}$ ,  $\text{CuSCN}$ , and  $\text{PTB7}$ ).

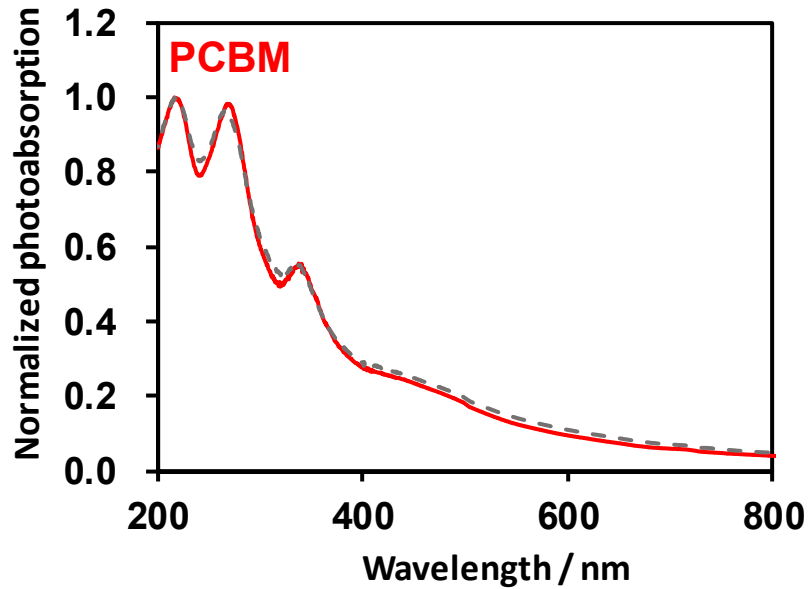


**Figure S4.** UV-visible photoabsorption spectra of PCBM film without EB (dotted line) and after EB exposure (solid red line).

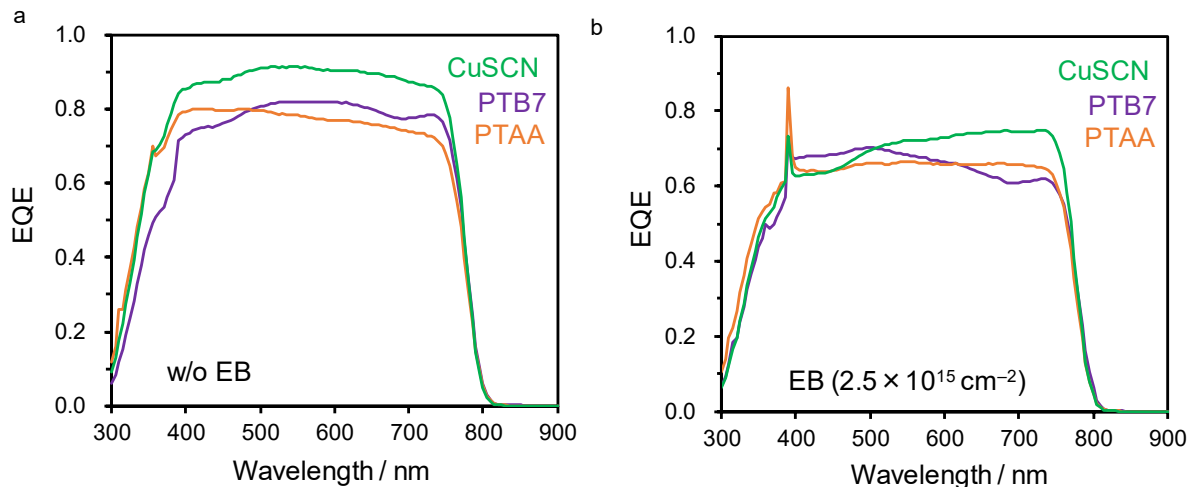


**Figure S5.** (a) EQE spectra of Device 4 (CuSCN), Device 5 (PTB7), and Device 6 (PTAA) without EB. Their maximum values are 0.92, 0.82, and 0.80, respectively. The onset is  $\sim 815$  nm. The  $J_{sc}$  calculated by integrating the EQE spectrum is 22.4, 20.0, and 19.5  $\text{mA cm}^{-2}$ , respectively. They are smaller than the  $J_{sc}$  under 1 sun (24.9, 24.2, and 25.7  $\text{mA cm}^{-2}$ , respectively). Note that the light intensities of our EQE instrument and solar simulator were calibrated by a standard cell, and a good match ( $<\pm 2\%$  difference) is obtained for organic solar cells. The small  $J_{sc}$  in EQE of PSC may be due to the trap filling under a stronger white light intensity of a solar simulator (our EQE facility does not provide a white light bias, and thus, the EQE is measured upon the exposure to a weaker intensity of light). (b) EQE spectra of Device 4 (CuSCN), Device 5 (PTB7), and Device 6 (PTAA) after EB exposure ( $2.5 \times 10^{15} \text{ cm}^{-2}$ ). The calculated  $J_{scs}$  are 18.1, 16.7, and 16.6  $\text{mA cm}^{-2}$ , respectively.

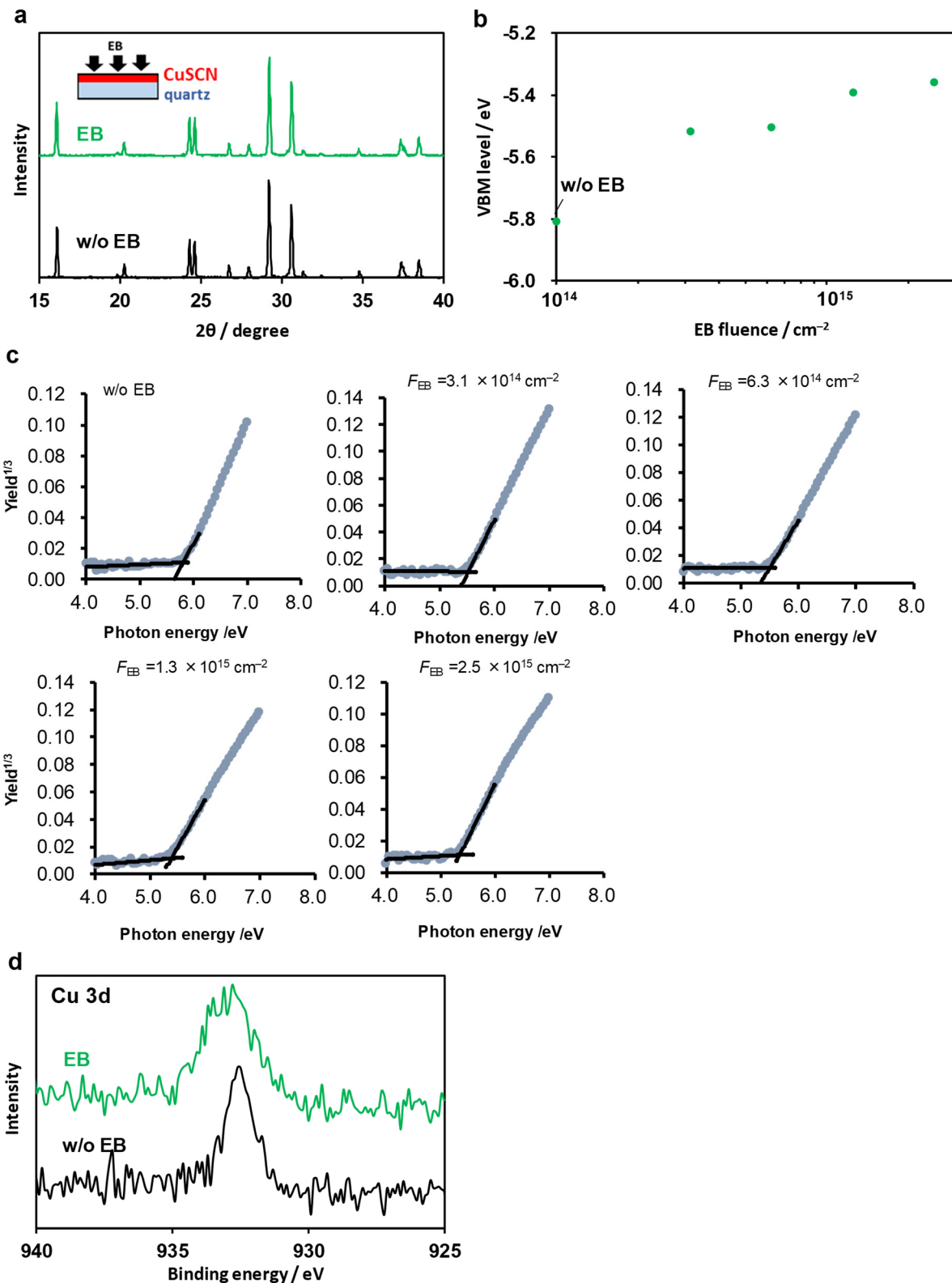


**Figure S6.** (a) XRD profiles of CuSCN without (black) and with EB ( $F_{EB} = 2.5 \times 10^{15} \text{ cm}^{-2}$ ) exposure. (b) VBM level of CuSCN after EB exposure. The point at  $F_{EB} = 10^{14} \text{ cm}^{-2}$  is the value without EB exposure. (c) PY spectra of CuSCN. The black lines are fitting to calculate the onset photon energy. (d) XPS profiles of Cu-3d states of CuSCN.

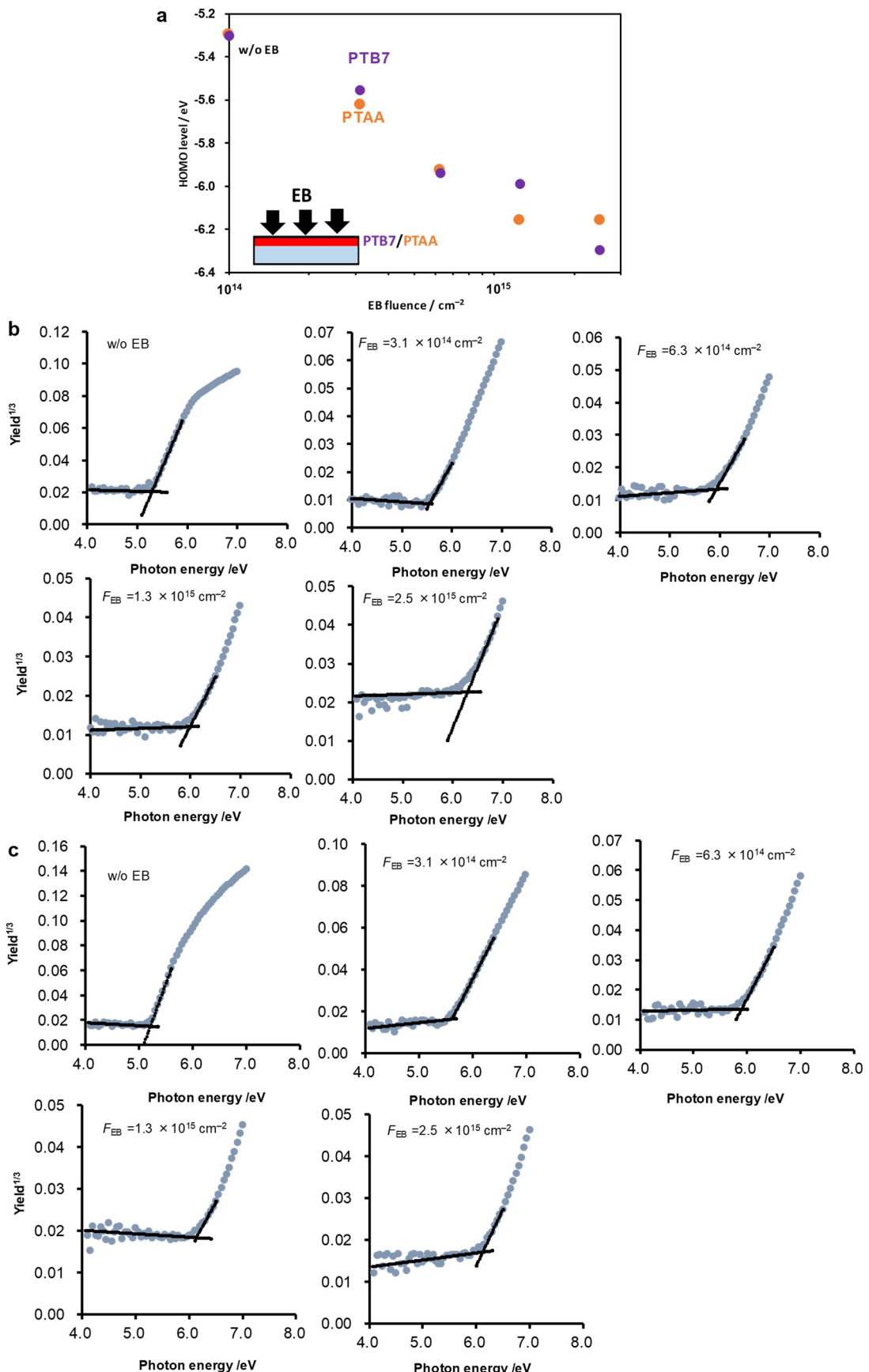


**Figure S7.** (a) HOMO level of PTB7 and PTA without EB exposure and after EB exposure, which was measured by PYS. (b) PY spectra of PTB7 with/without EB. (c) PY spectra of PTA with/without EB.

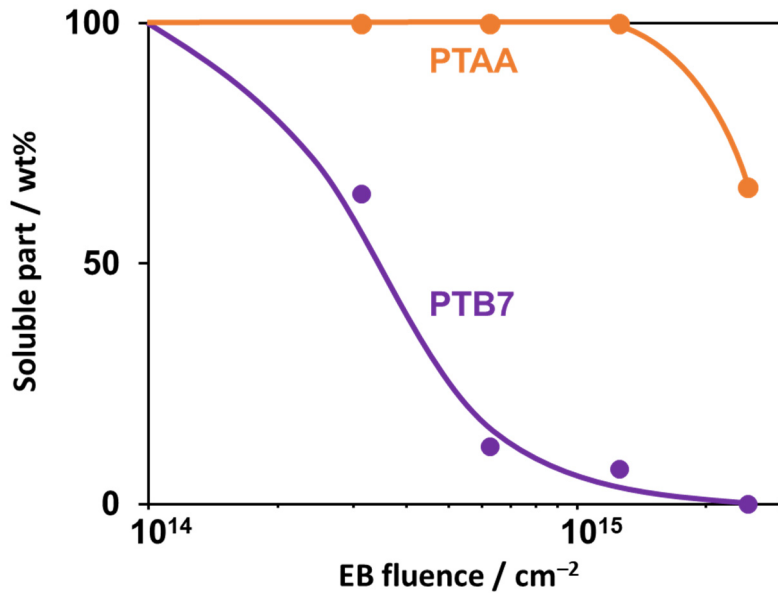


**Figure S8.** Weight fraction of soluble part of PTB7 and PTAA in chloroform after EB exposure.

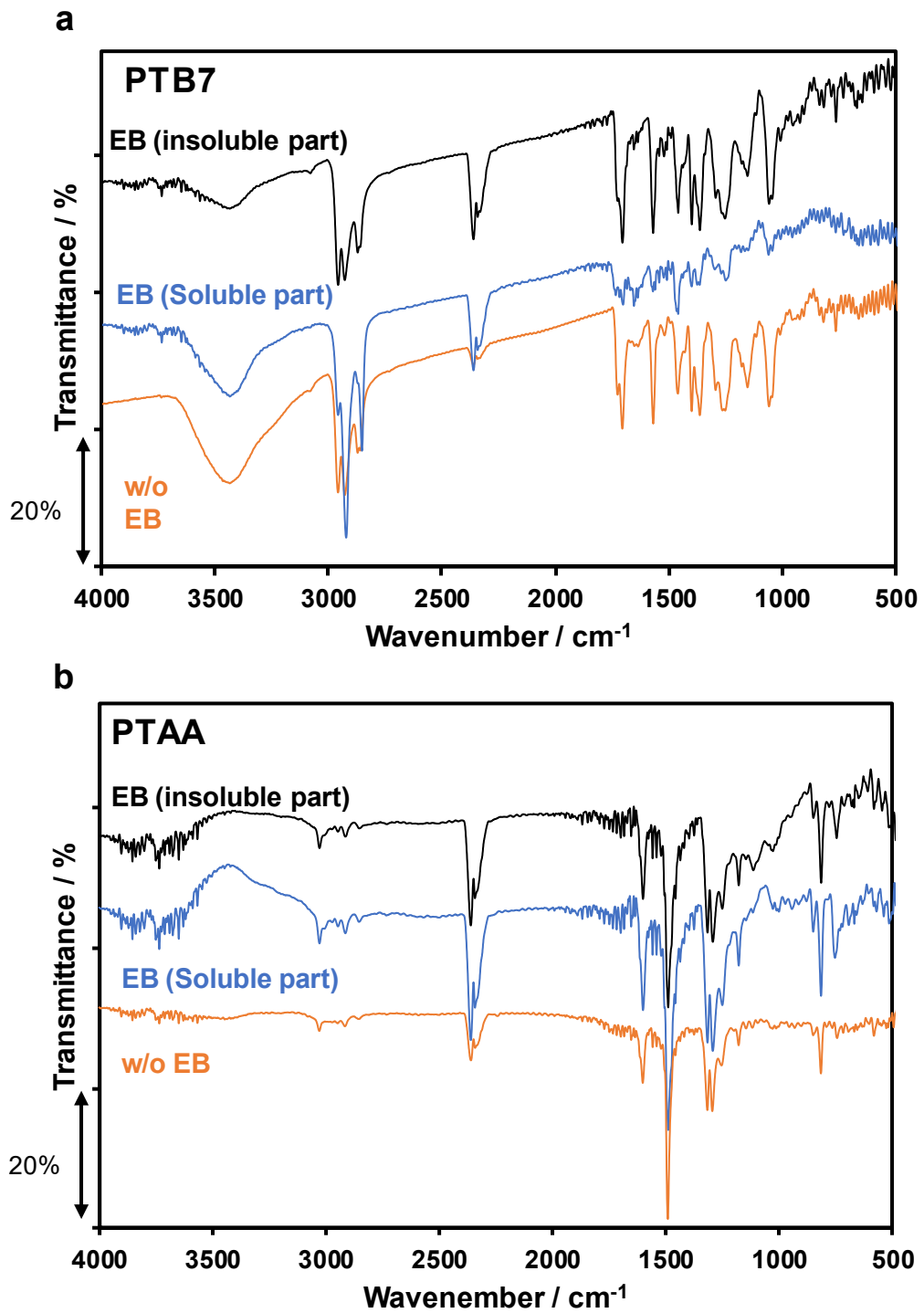


**Figure S9.** FT-IR spectra (KBr) of (a) PTB7 ( $F_{\text{EB}} = 3.1 \times 10^{14} \text{ cm}^{-2}$ ) and (b) PTAA ( $F_{\text{EB}} = 2.5 \times 10^{15} \text{ cm}^{-2}$ ).

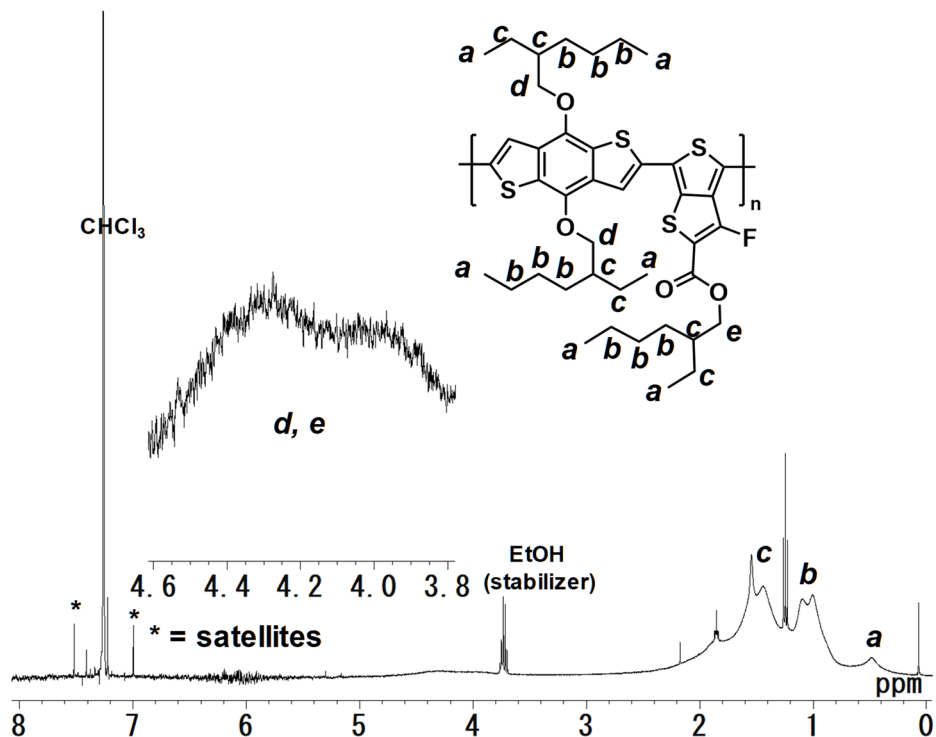


**Figure S10.** NMR chart of PTB7 without EB exposure (400 MHz, CDCl<sub>3</sub>, 25 °C).

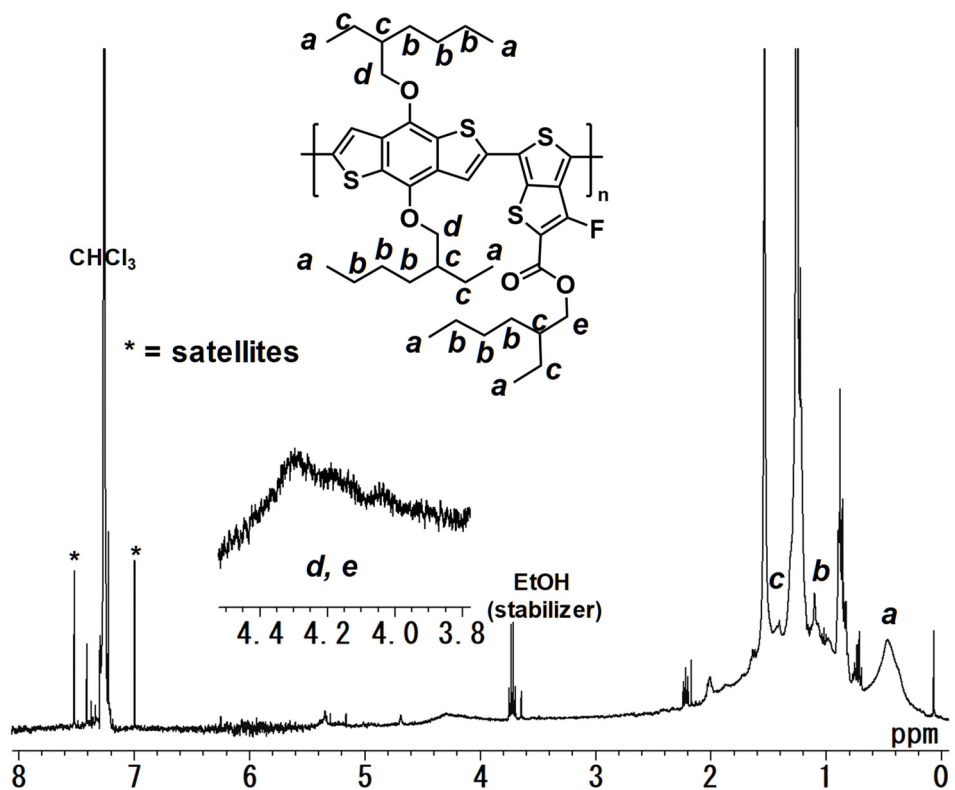


**Figure S11.** NMR chart of PTB7 and after 2.5 × 10<sup>15</sup> cm<sup>-2</sup> EB exposure (400 MHz, CDCl<sub>3</sub>, 25 °C).

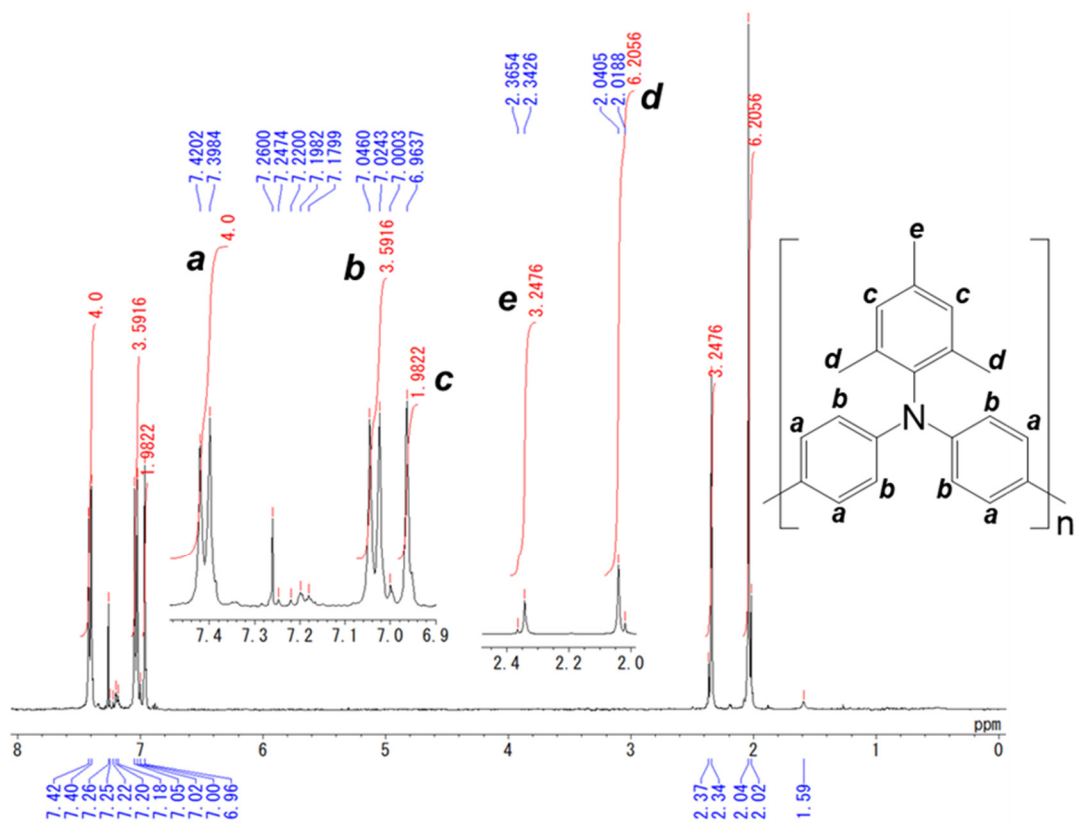


**Figure S12.** NMR chart of PTAA without EB exposure (400 MHz, CDCl<sub>3</sub>, 25 °C).

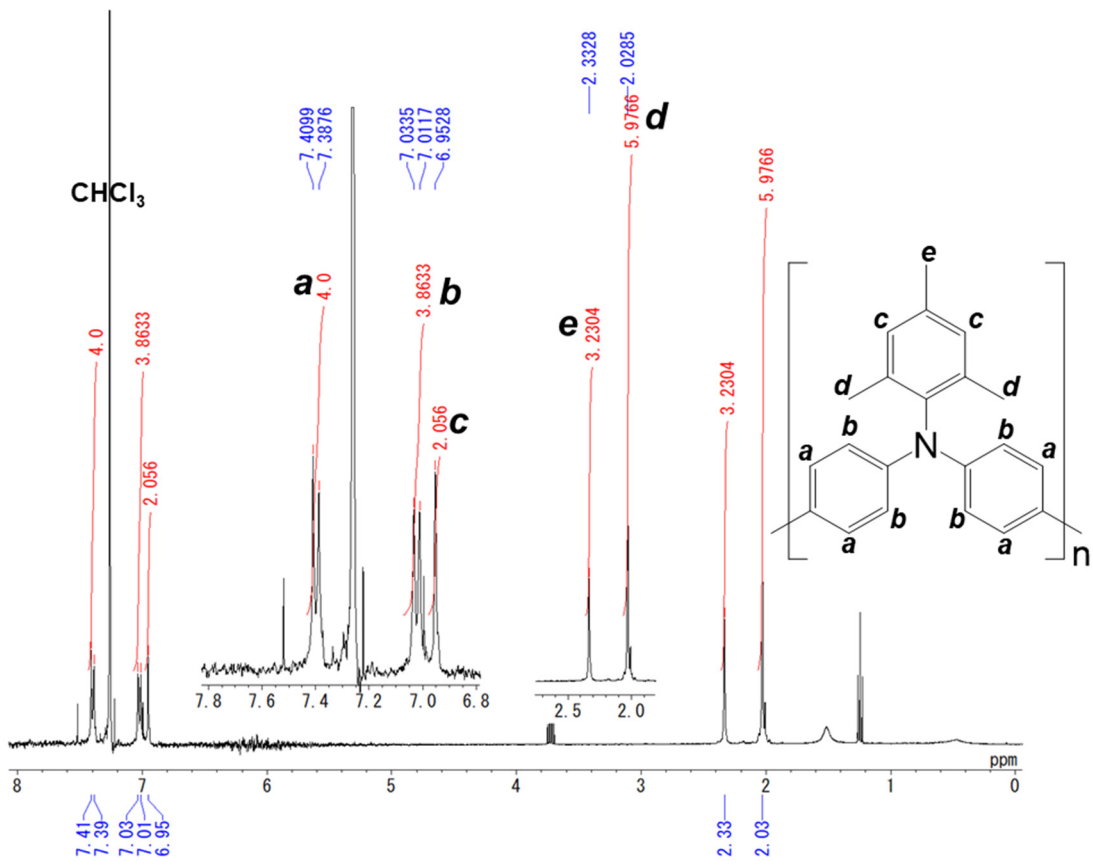


**Figure S13.** NMR chart of PTAA after  $2.5 \times 10^{15} \text{ cm}^{-2}$  EB exposure (400 MHz,  $\text{CDCl}_3$ , 25 °C).

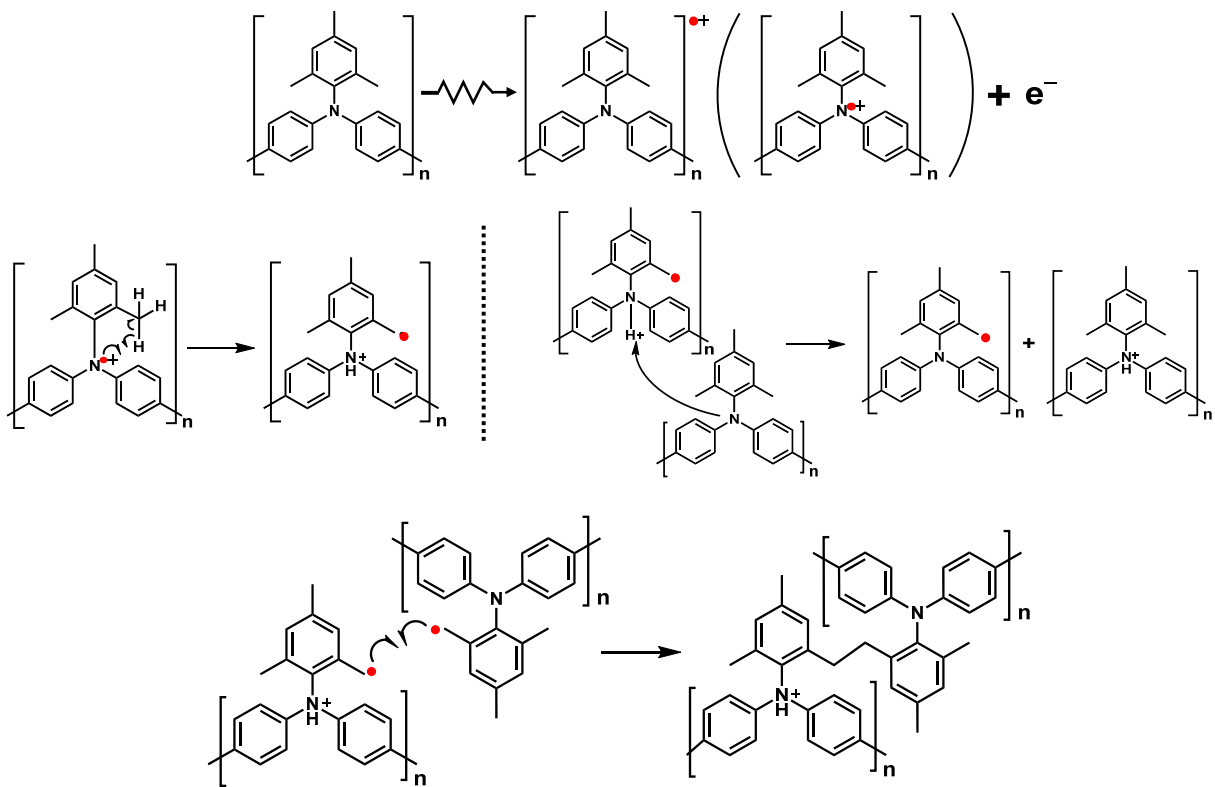


**Figure S14.** Possible mechanism of PTAA crosslinking upon EB exposure. The radical is illustrated by the red circles.

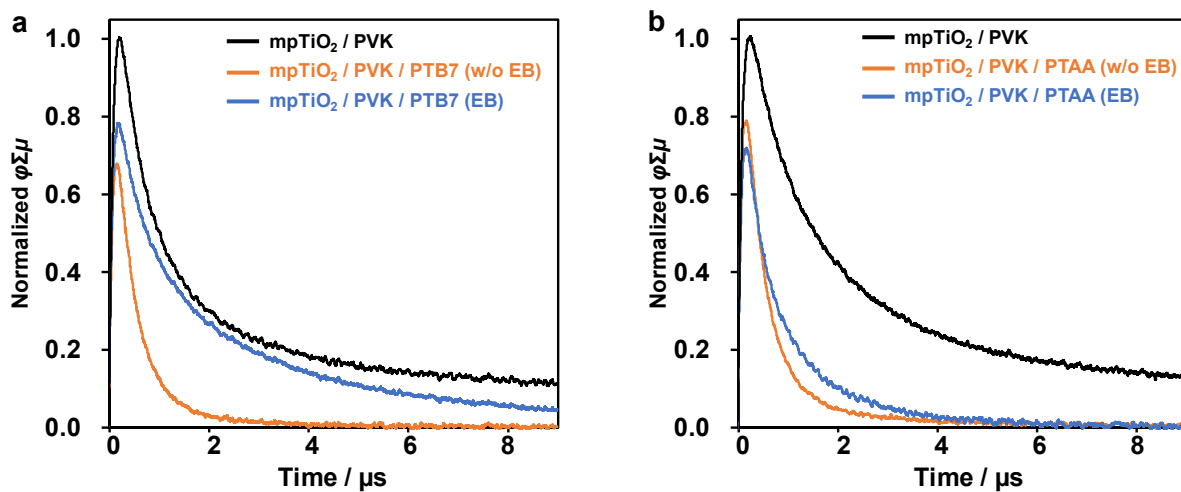


**Figure S15.** Normalized TRMC transients ( $\lambda_{\text{ex}} = 500 \text{ nm}$ ) of (a) mp-TiO<sub>2</sub> / PVK / PTB7 (b) mp-TiO<sub>2</sub> / PVK / PTAA ( $F_{\text{EB}} = 2.5 \times 10^{15} \text{ cm}^{-2}$ ).

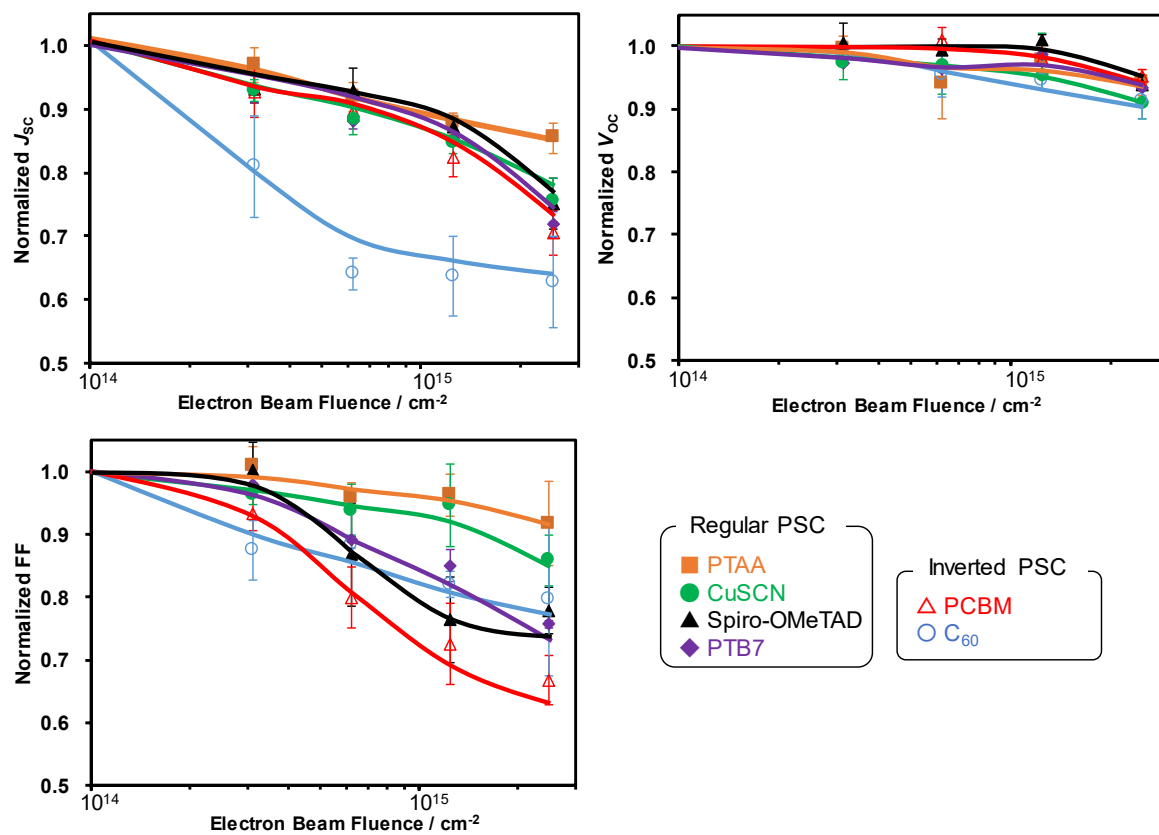


**Figure S16.** Normalized values of  $J_{SC}$ ,  $V_{OC}$ , and fill factor.

### **Supplementary references**

(S1) N. Ishida, A. Wakamiya and A. Saeki, *ACS Photonics* 2016, **3**, 1678.